The Journal of Experimental Biology 213, 1281-1292

doi:10.1242/jeb.037200

Morphology–flow interactions lead to stage-selective vertical transport of larval sand dollars in shear flow

T. W. Clay* and D. Grünbaum

University of Washington, UW School of Oceanography, Box 357940, Seattle, WA, USA

*Author for correspondence (tansy@u.washington.edu)

Accepted 2 January 2010

SUMMARY

Many larvae and other plankton have complex and variable morphologies of unknown functional significance. We experimentally and theoretically investigated the functional consequences of the complex morphologies of larval sand dollars, *Dendraster excentricus* (Eschscholtz), for hydrodynamic interactions between swimming and turbulent water motion. Vertical shearing flows (horizontal gradients of vertical flow) tilt organisms with simple geometries (e.g. spheres, ellipsoids), causing these organisms to move horizontally towards downwelling water and compromising their abilities to swim upwards. A biomechanical model of corresponding hydrodynamic interactions between turbulence-induced shear and the morphologically complex four-, six- and eight-armed stages of sand dollar larvae suggests that the movements of larval morphologies differ quantitatively and qualitatively across stages and shear intensities: at shear levels typical of calm conditions in estuarine and coastal environments, all modeled larval stages moved upward. However, at higher shears, modeled four- and eight-armed larvae moved towards downwelling, whereas six-armed larvae moved towards upwelling. We also experimentally quantified larval movement by tracking larvae swimming in low-intensity shear while simultaneously mapping the surrounding flow fields. Four- and eight-armed larvae moved into downwelling water, but six-armed larvae did not. Both the model and experiments suggest that stage-dependent changes to larval morphology lead to differences in larval movement: four- and eight-armed stages are more prone than the six-armed stage to moving into downwelling water. Our results suggest a mechanism by which differences can arise in the vertical distribution among larval stages. The ability to mitigate or exploit hydrodynamic interactions with shear is a functional consequence that potentially shapes larval evolution and development.

Key words: biomechanics, evolution of shape, functional morphology, hydrodynamic model, larval development, larval swimming.

INTRODUCTION

In many species of benthic marine invertebrates, a planktonic larval stage plays an important role in long-range transport between otherwise-isolated populations and between existing populations and unoccupied habitats (Cowen and Sponaugle, 2009; Hunt, 1993; Scheltema, 1986; Shanks et al., 2003). The vertical distributions of planktonic larvae in the water column often strongly influence their survival and dispersal because key biotic and abiotic environmental characteristics vary rapidly with depth. The vertical positions of larvae are determined in part by advection in turbulence and ambient currents but, in many species, are also strongly influenced by larval swimming. In most planktonic larvae, little is known about the biomechanical limits to overall swimming performance or the behavioral mechanisms that determine how swimming capabilities are utilized. Our poor understanding of larval swimming characteristics and the implications of larval swimming for dispersal is currently a serious limitation on ecological analysis and management of many benthic marine populations.

Previous investigations of larval swimming have generally focused on performance in still water (Chia et al., 1984; Emlet, 1990; Emlet, 1991; Emlet, 1994; Higgins et al., 2008; McHenry, 2005; Pennington and Strathmann, 1990). A limitation of using still-water performance to assess larval transport in shears, turbulence and other flows is that both larval behavior and swimming performance can be altered by water movement. Hence, larval movement is not simply a sum of independent advection and swimming components. Larval behavioral responses to flow are not well understood and have been described for only a few species. For example, Fuchs and colleagues (Fuchs et al., 2004) described behaviors of gastropod larvae in turbulence, Pawlik and Butman (Pawlik and Butman, 1993) examined the effects of hydrodynamics on the settlement behavior of larval tubeworms, and Koehl and Reidenbach (Koehl and Reidenbach, 2007) and Hadfield and Koehl (Hadfield and Koehl, 2004) investigated the effects of chemical cues on larval nudibranch behavior in turbulence and ambient water flow. The biomechanical effects of flow on larval swimming, in particular how flow directly affects swimming performance and how variations in larval morphology translate into differential movements in flow, are even less well understood.

As they move within the water column, larvae typically experience spatially and temporally fluctuating levels of shear and turbulence (Yamazaki et al., 2002). Typical oceanic turbulent energy dissipation rates range from 10^{-6} to $10^{0}\,cm^{2}\,s^{-3}$ (Kiøerboe and Saiz, 1995). The Kolmogorov scale, which indicates the approximate characteristics of turbulent eddies, suggests that the smallest turbulent eddies associated with these dissipation rates are on the order of 1 to 0.03 cm in length, 0.01 to 0.3 cm s^{-1} in velocity, and 100 to 0.10 s in duration (Kundu and Cohen, 2002; Tennekes and Lumley, 1972; Yamazaki et al., 2002). The ratio of the velocity to length scales for these energy dissipation rates suggests shears on the order of 0.01 to 10 s^{-1}.

Ciliated invertebrate larvae range typically from approximately 100 μm to 1 mm in length and swim at velocities up to approximately 10 mm s^{-1} (Emlet, 1991). Hence, except under the most energetic

oceanic conditions, larval sizes and velocities are typically comparable to or smaller than those of the smallest turbulent eddies. Therefore it is likely that, for a large fraction of their planktonic period, larvae experience their immediate turbulent surroundings as a succession of shear flows.

Previous work has suggested that many geotactic (up-swimming) algae, larvae and other plankton in vertical shearing flows (i.e. horizontal gradients in vertical velocities) are tilted towards downwelling water (Kessler, 1985; McDonald, 2007; Strathmann and Grünbaum, 2006). Shear is made up of vorticity and pure strain. This tilting occurs because the vorticity component of the shear flow rotates planktonic organisms in the direction of downwelling water. This off vertical inclination causes planktonic organisms that are swimming to cross streamlines selectively into downwelling water. Because simple morphologies such as spheres and ellipsoids move in this way, movement into downwelling water can be regarded as the 'default' response to shear by passively stable plankton. The consequences of this can include bioconvection, the self-generated circulatory flows often observed in tidal pools and unstirred larval or algal cultures, hydrodynamic focusing, in which gyrotaxis and hydrodynamic torque combine to concentrate cells into a column, and gyrotactic trapping, in which vertical migration is disrupted by hydrodynamic shear (Bearon and Grünbaum, 2006; Durham et al., 2009; Kessler, 1985; Pedley and Kessler, 1992a; Pedley and Kessler, 1992b). For up-swimming larvae, movement into downwelling water potentially compromises control over vertical movements and ultimately their distribution in the water column.

More-specialized larval morphologies could in theory allow movement in the opposite direction, into upwelling water. If so, such larvae might be advected upward at velocities much greater than their swimming velocities. For these larvae, the presence of shear might enhance rather than compromise the effectiveness of up-swimming. However, larvae with this type of interaction with flow have not been reported.

The focus of this study is on 'armed' larval morphologies, in which long, thin, ciliated protrusions extend from the body to provide propulsion and capture food (Grünbaum and Strathmann, 2003). Examples include the pluteus larvae of ophiuroids and echinoids, phoronid larvae, some mollusc larvae such as larvae of the hairy triton, and some larval annelids, including those with the rostraria larval form. The repeated evolution of armed larvae in these diverse taxonomic groups suggests the hypothesis that these forms provide biomechanical advantages in swimming or feeding.

Larval swimming performance is determined by larval morphological characteristics such as size, shape and mechanisms of propulsion (Chia et al., 1984; Emlet, 1990; Emlet, 1991; Emlet, 1994; Grünbaum and Strathmann, 2003; Higgins et al., 2008; McHenry, 2005; Pennington and Strathmann, 1990; Strathmann and Grünbaum, 2006). Despite broad similarities in armed larvae, morphological details such as arm number, length and orientation vary strongly both across and within taxa (McEdward, 1984; McEdward and Herrera, 1999; Young et al., 2002). In the context of swimming, this high degree of morphological diversity is open to multiple interpretations. Diversity could be high because variations in morphological parameters have weak functional consequences for swimming performance. Alternatively, morphological diversity among armed larvae might reflect very strong functional consequences: if one morphological feature changes, others might also require adjustment to avoid serious compromises in swimming abilities.

In a previous study, the results of a hydrodynamic model of swimming in armed larvae suggested that the observed variations in armed larval morphologies do indeed have significant consequences for swimming performance (Grünbaum and Strathmann, 2003). The metrics of swimming performance in that study were swimming speed, weight-carrying ability and hydrodynamic stability in shear. In a systematic investigation of idealized larval morphologies, no single morphology optimized all of the swimming performance criteria examined. Lack of a single overall optimal morphology suggests that trade-offs exist, for example, between morphologies that are highly stable and those that swim fastest or carry the most weight (Grünbaum and Strathmann, 2003; Strathmann and Grünbaum, 2006).

The larvae of *Dendraster excentricus*, a sand dollar, develop through several pluteus morphologies, progressing through four-armed, six-armed and, finally, eight-armed stages. The primary morphological differences between these stages, in addition to arm number, are increases in larval size and arm length. Environmental conditions can also affect *Dendraster* larval morphology. For example, starved *Dendraster* larvae have relatively long arms, whereas well-fed larvae have shorter arms (Boidron-Metairon, 1988; Hart and Strathmann, 1994). The general consistency between *Dendraster* larval morphologies and assumptions in Grünbaum and Strathmann's (Grünbaum and Strathmann, 2003) hydrodynamic model presents an opportunity to apply both empirical and theoretical approaches to investigate *Dendraster* swimming. *Dendraster* are also thought to lack gravity-sensing organs such as statoliths, suggesting that they lack a sensory basis for active orientation control. This is consistent with assumptions of the model, which do not allow for active behavioral responses to hydrodynamic signals.

In this study, *Dendraster* was used as a focal species to investigate empirically and theoretically how hydromechanical interactions between larval morphology and ambient shear flows affect larval movement. A detailed hydrodynamic model of *Dendraster* larvae was developed that predicts swimming performance in shear flows from first-principles based on specific morphological assumptions. A morphological analysis of four-, six- and eight-armed *Dendraster* larvae was conducted that provided parameters for the hydrodynamic model. Quantitative observations of *Dendraster* larvae swimming in manipulated shear fields were made, which served as partial comparisons for predictions of the model. Swimming observations were based on a video-tracking method in which larval movements were reconstructed simultaneously with particle tracking velocimetry (PTV) to quantify the velocity field in the surrounding water.

MATERIALS AND METHODS

Larval culture

Adult sand dollars (*Dendraster excentricus* Eschscholtz) were collected from East Sound, Orcas Island, WA, USA and were spawned and fertilized using standard techniques (Strathmann, 1987). Larvae were cultured in 2.5-liter jars (approximately two larvae per ml) in bag-filtered (5 μm) water under continuous gentle stirring. Water changes and feeding with *Rhodomonas lens*, at a concentration of approximately 5000 cells ml^{-1}, took place 12–24 h post-fertilization and 2–3 times per week thereafter.

Morphometrics

Four-, six- and eight-armed larvae from shear and swimming experiments were preserved in a 70% ethanol and seawater solution buffered (supersaturated) with sodium bicarbonate. Approximately 30 individuals from each experimental date were photographed under conditions of 10× magnification. Larvae lying either dorsal or ventral side up were included for most morphometrics, resulting

in measurements from 31 four-armed, 29 six-armed and 31 eight-armed individuals. Only larvae lying ventral side up were used to quantify the length and position of the preoral and posterodorsal arms, giving sample sizes of 10 and 9 individuals for six- and eight-armed stages, respectively (Fig. 1). Four-armed larvae lack preoral and posterodorsal arms.

The maximum distance between the postoral and anterolateral arms and the distance from the anterolateral arms to the tips of the preoral and posterodorsal arms were measured for each larva using the fine-adjustment knob on the microscope, which had been calibrated previously with a capillary tube of known diameter. Posterodorsal arms were coplanar with the anterolateral arms in all larvae. Other morphological measurements were digitized from the photographs with the image-analysis software ImageJ version 1.36b (NIH) and calibrated with photographs of a stage micrometer (Fig. 1) (Clay, 2008): arm length (extending from arm tip to the posterior end of the larval body), diameter of the postoral and anterolateral arms at the arm tip, distance between the tips of the two arms within each pair, and body height (the distance between the posterior end of the larval body and the ventral transverse band at the midline of the larva). Skeletal rods were intact in all preserved specimens, but there was a small amount of tissue shrinkage. In a few animals, tissue did not extend to the tip of the skeletal rod owing to imperfect fixation. For these larvae, the arm tip was assumed to have extended originally to the tip of the skeletal rod. The actual lengths of larval body parts that were not lying flat against the slide were calculated from the maximum distance between the postoral and anterolateral arms and observed projected lengths.

To calculate body volume, the body was approximated as an inverted pyramid, with edges running up the sides of the arms and extending to the low-point of the ventral transverse band between the post-oral arms (Fig. 1) (Clay, 2008). The upper limit of the body on the anterolateral face of the pyramid was assumed to be equal to that on the postoral face. Hydrodynamic model calculations were based on averages of morphological parameters for each larval stage.

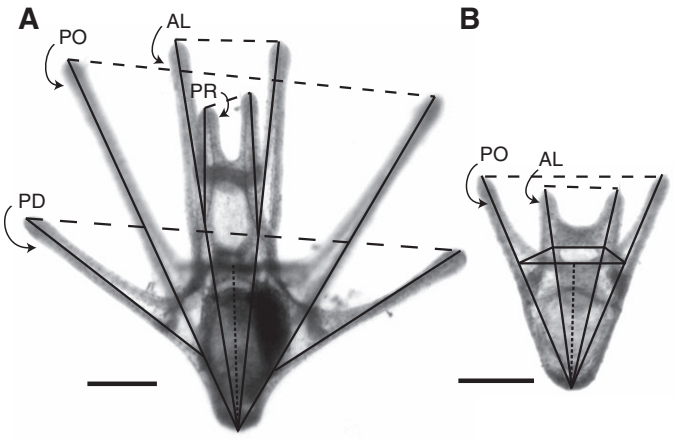

Fig. 1. Measurements from larvae used to parameterize the model. (A) An eight-armed larva, illustrating how larval morphology was quantified. (B) A four-armed larva, along with the pyramid-shaped larval body assumed in the model. For both images, solid lines represent measurements of arm length, dashed lines represent measurements of width between tips within an arm pair, and the dotted line represents the measurement for body height. One arm in each pair is labeled: postoral arms (PO), anterolateral arms (AL), posterodorsal arms (PD) and preoral arms (PR). Scale bars, 100 μm.

Metrics of larval movement

Three metrics were used to summarize larval movement in the model and the experiments. Relative vertical velocity (v) was defined as the total vertical velocity of a larva minus the vertical velocity of the surrounding fluid. Relative horizontal velocity (u) was defined analogously for the horizontal movement projected onto the x–y plane. The third metric, net vertical velocity (v_{net}), quantified how much horizontal movement towards upwelling or downwelling water affected actual vertical movements. To quantify net vertical velocity, the change in position over a time interval t of a larva with initial position x=y=0 and embedded in a uniform shear flow was modeled as:

$$Y(t) - 1/2aut^2 + vt\,. \quad (1)$$

In Eqn 1, the ambient vertical flow velocity is V=ax, and the horizontal flow velocity is zero. The first term on the right side of the equation represents vertical advection of the larva, which is dependent upon the vertical flow velocity (V=ax) and the time a larva is exposed to that flow (t). The x position of the larva is dependent upon the horizontal velocity of the larva and the time it moves at that velocity (ut). A constant u was assumed, so that the average vertical flow velocity a larva was exposed to over the time interval (t) was half the vertical flow velocity at time (t). Eqn 1 makes explicit the dependence of larval movement on time, relative vertical velocity, relative horizontal velocity and shear. Using Eqn 1, v_{net} was defined as the mean vertical movement rate, v_{net}=$y(t)/t$, for a specific choice of time interval t. Results are reported for t=20 s because this time-interval falls in the middle of the range of Kolmogorov time-scales for the relevant range of dissipation rates and so might be a reasonable indicator of how long larvae experience an approximately constant level of shear (Yamazaki et al., 2002). All three metrics were used for statistical analysis.

Modeling

Our hydrodynamic model was modified from the low-Reynolds-number slender-body model of Grünbaum and Strathmann (Grünbaum and Strathmann, 2003). The model used here was dimensional rather than nondimensional and was parameterized using larval morphologies observed in this study. The geometries of postoral and anterolateral arm pairs were specified in the model by arm sweep angle and arm elevation angle (Figs 2 and 3) (Clay, 2008). For six- and eight-armed larvae, preoral and posterodorsal arms were added with geometries specified by positions of the start and tip of each arm relative to the anterolateral and postoral arms. Bilateral symmetry was assumed between the two arms within each pair. First-order fluid effects of a larval body were approximated by adding non-ciliated cylinders along the edges of the body. The base of the pyramid was constrained by the three-dimensional position of the arms, and the height was constrained by the larval body volume, which was calculated from morphological data. The positions of the gravitational and buoyant forces and their magnitudes were calculated explicitly from the distributions of tissue and skeleton mass (Clay, 2008).

Some model parameters could not be measured directly in this study. Skeleton volume was estimated for four-armed larvae to be approximately 6%, based on reported estimates that the skeleton of these plutei contributes as much as 77% of their excess density (Pennington and Emlet, 1986; Pennington and Strathmann, 1990) and assuming that the skeleton density was 2.71 g ml^{-1}, the same as mineral calcite (Clay, 2008). The model used here did not explicitly model ciliary action but instead assumed a ‘traction velocity’ at the ciliated surfaces of larval arms (for details, see Grünbaum and Strathmann,

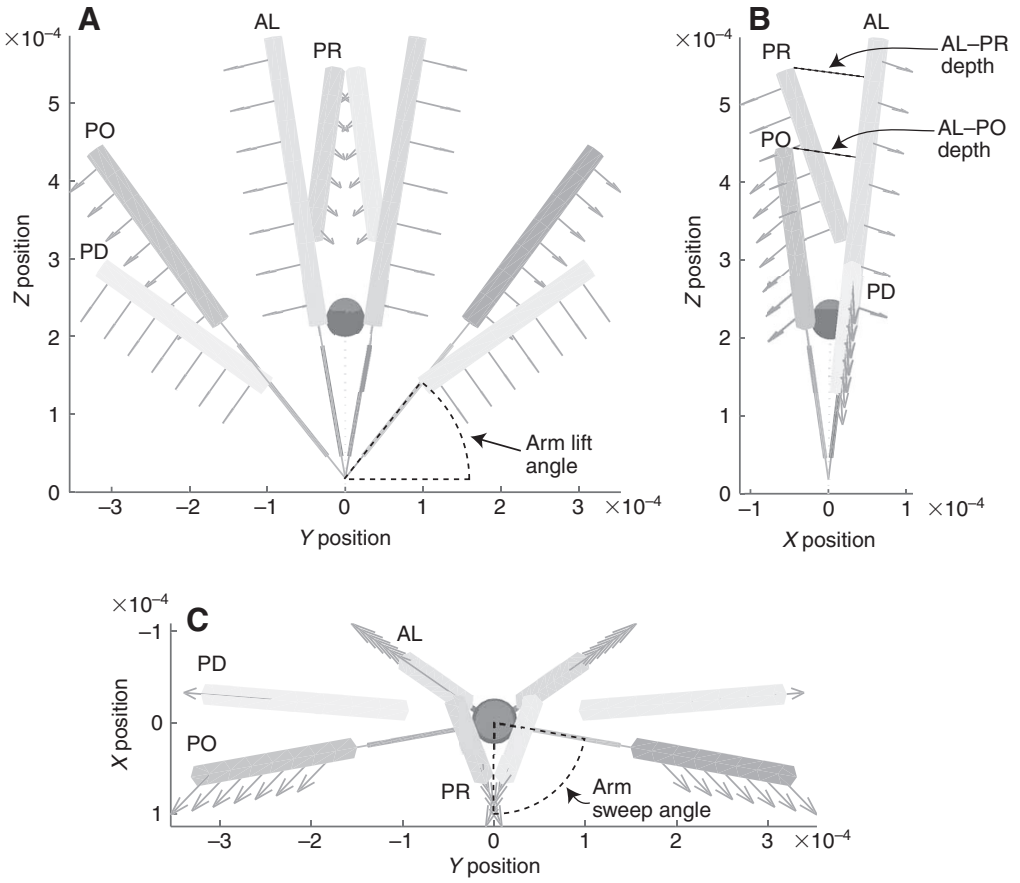

Fig. 2. Schematic diagrams of model eight-armed larva illustrating model parameters on a front view (A), side view (B) and top view (C). Thicker cylinders represent ciliated portions of larval arms, and arrows extending perpendicularly from larval arms represent the direction of ciliary forces. Thinner cylinders represent the larval body. Model parameters are designated with dashed lines. One arm in each pair is labeled: postoral arms (PO), anterolateral arms (AL), posterodorsal arms (PD) and preoral arms (PR).

2003). This traction velocity is not equivalent to ciliary tip speed and so could not be observed directly. In the model used here, the traction velocity was adjusted to make the swimming speed of model larvae in still water match experimental observations (Clay, 2008). The resulting traction velocity was greater than reported values for velocities near ciliary tips, which is expected because the modeled traction velocity acts at the bottom of the cilia. The propulsive force was assumed to be directed in the plane containing the z-axis and the larval arm and perpendicular to the larval arm. In postoral arms of six- and eight-armed larvae, the propulsive force on the postoral arms was perpendicular to the arms but rotated towards the ventral side of the larva by $\pi/6$ radians relative to the plane containing the z-axis and the larval arm (Figs 2 and 3). Larvae with the propulsive force on the postoral arms rotated in this way matched observations for swimming in still water (Clay, 2008).

Swimming of each larval stage in simple vertical shear flow was modeled for 16 shear levels, ranging from 0 to 10 s^{-1}. To minimize bias owing to initial orientation, 128 random initial orientations were chosen. This same set of 128 initial orientations was then used for each stage at each shear level. After simulating larval swimming for 100 s to allow initial transients in orientation to subside, larval movement was measured for 20 s. Median, tenth and ninetieth percentiles for all three metrics of larval movement are reported. Median velocities are reported because in some cases the distributions were skewed.

Experiments

Swimming performance of four-, six- and eight-armed *Dendraster* larvae in shear was quantified within a 5×1×7 cm observation tank. *Rhodomonas lens* cells, which were nearly neutrally buoyant, were also added to the tank as flow tracer particles. For *Rhodomonas* sp., average swimming velocities of 85 μm s^{-1} (Sheng et al., 2007) and sinking velocities of 0.07 m day^{-1} (Burns and Rosa, 1980) have been reported. Vertical shear was generated in this tank using temperature differences between opposing sides (Fig. 4) (Strathmann and Grünbaum, 2006). Video tracking was used both to quantify two-dimensional larval movements and to determine shear field distributions (Figs 4 and 5).

Imaging, video acquisition and processing

The experimental tank was illuminated from above with visible light from an incandescent microscope lamp. Larvae and algae were imaged with a Cohu 4815-3000/000 camera and a Nikon 60 mm Micro Nikkor lens. The lens was focused in the center of the tank and was positioned 15 cm from the front of the experimental tank. All video was recorded with a Panasonic SVHS AG-1980 Proline Desktop Editor and later captured to a computer with either a Sony DVMC-DA1 Media Converter or a Sony DSR-20 DVCAM and Kino video editing software. Video segments were processed on a Linux work station using a version of the open-source video editor avidemux2 customized for motion analysis. To minimize wall effects, video was cropped to include only the middle 90% of the back face of the experimental chamber. Larvae and algal cells could be reliably distinguished by the processing algorithms based on size and brightness. Using these criteria, the avidemux2 analysis was run twice, tracking larvae in one pass and algal cells in the other. Video was de-interlaced, background-subtracted and thresholded. Particles and larvae were then identified as contiguous groups of above-threshold pixels, and their pixel coordinates in each video frame were recorded. Particle positions in sequential frames were

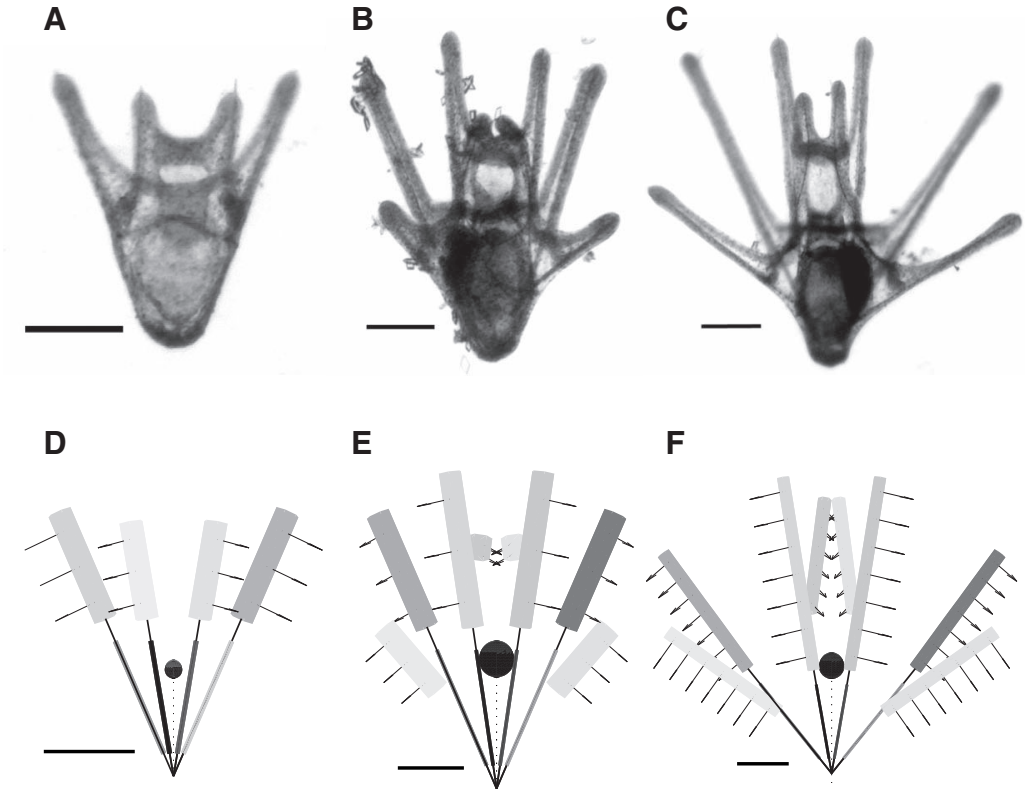

Fig. 3. Larval *Dendraster excentricus* at the four- (A), six- (B) and eight-armed (C) stages. Schematic of larval model parameterized with average measurements of four- (D), six- (E) and eight-armed (F) larvae. Buoyant and gravity forces are represented by light- and dark-gray spheres, respectively, with sphere position indicating the center of each force (X_{buoy} and X_{grav}, respectively) and sphere size representing the magnitude of each force (F_{buoy} and F_{grav}, respectively). For four-armed larvae, F_{buoy}=[0, 0, 0.8818]×10^{-8}, X_{buoy}=[–0.0017, 0, 0.1293]×10^{-3} and F_{grav}=[0, 0, –0.9334]×10^{-8}, X_{grav}=[–0.0019, 0, 0.1277]×10^{-3}. For six-armed larvae, F_{buoy}=[0, 0, 0.2516]×10^{-7}, X_{buoy}=[0.0036, 0, 0.1908]×10^{-3} and F_{grav}=[0, 0, –0.2637]×10^{-7}, X_{grav}=[0.0034, 0, 0.1878]×10^{-3}. For eight-armed larvae F_{buoy}=[0, 0, 0.2262]×10^{-7}, X_{buoy}=[0.0025, 0, 0.2267]×10^{-3} and F_{grav}=[0, 0, –0.2419]×10^{-7}, X_{grav}=[0.0023, 0, 0.2230]×10^{-3}. Lines extending perpendicular to the larval arms represent the direction of ciliary propulsion. Scale bars, 100 μm.

converted into physical dimensions using calibration images of a ruler in known positions and assembled into intact trajectories with in-house Matlab-based software (Tracker3D; Fig. 4).

Shear experiments

Shear levels were controlled by adjusting circulating water baths that controlled the temperature on each side of the tank. After temperature adjustments, five minutes were allowed to establish steady vertical shear flow and for larvae to re-acclimate before videotaping began. Shear was then temporally constant, although still spatially non-uniform within each shear treatment (Fig. 5). Temperature in the center of the tank was measured before and after filming at each shear level to confirm that it remained constant at 11°C within the tank, outside of the temperature and velocity boundary layers.

The steady-state flow-field for each shear setting was quantified with two minutes of algal trajectories (typically 10,000 to 40,000 tracks), usually from minutes 9–11 of each 20-min shear treatment. Occasionally, the tank was stirred during that time interval to redistribute the larvae, in which case the timing was adjusted slightly to ensure that the regular flow was quantified (Clay, 2008). Algal trajectories from Tracker3D were processed to extract flow-fields by calculating median velocities within a 19×20 array of bins spanning the region of interest. Temperature differences across the tank of 2°C and 4°C (10–12°C and 9–13°C) resulted in shears ranging from approximately –0.05 to 0.24 s^{-1} and –0.05 to 0.41 s^{-1}

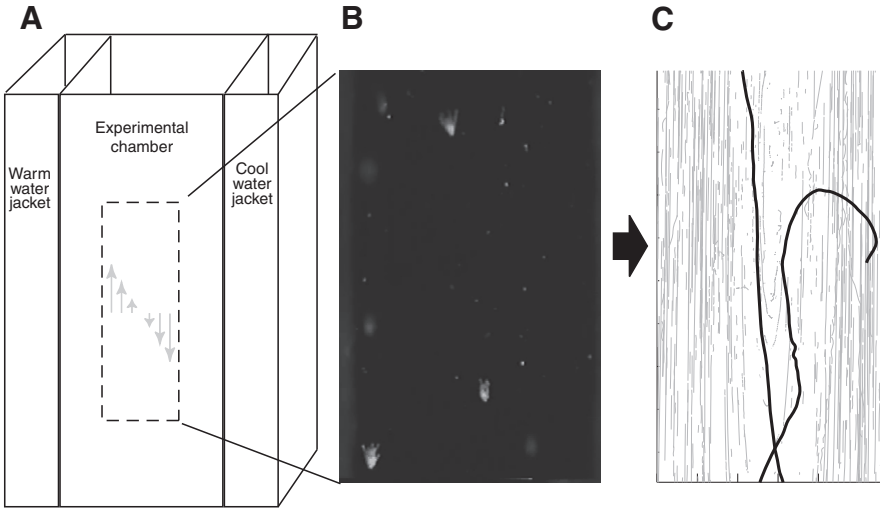

Fig. 4. Experimental set-up. Shear was driven in the experimental tank by temperature differences at the walls of the experimental chamber created by water baths on either side of the tank (A). Arrows represent flow within the tank, and the dashed rectangle represents the camera's field of view. A video frame from the experimental chamber (B) illustrates how larvae and tracer particles could be reliably distinguished based on size and brightness. Representative trajectories of tracer particles (gray lines) and larvae (black lines) resulting from video analysis (C) show how tracer particles define the flow-field and how larval trajectories deviate from ambient flows.

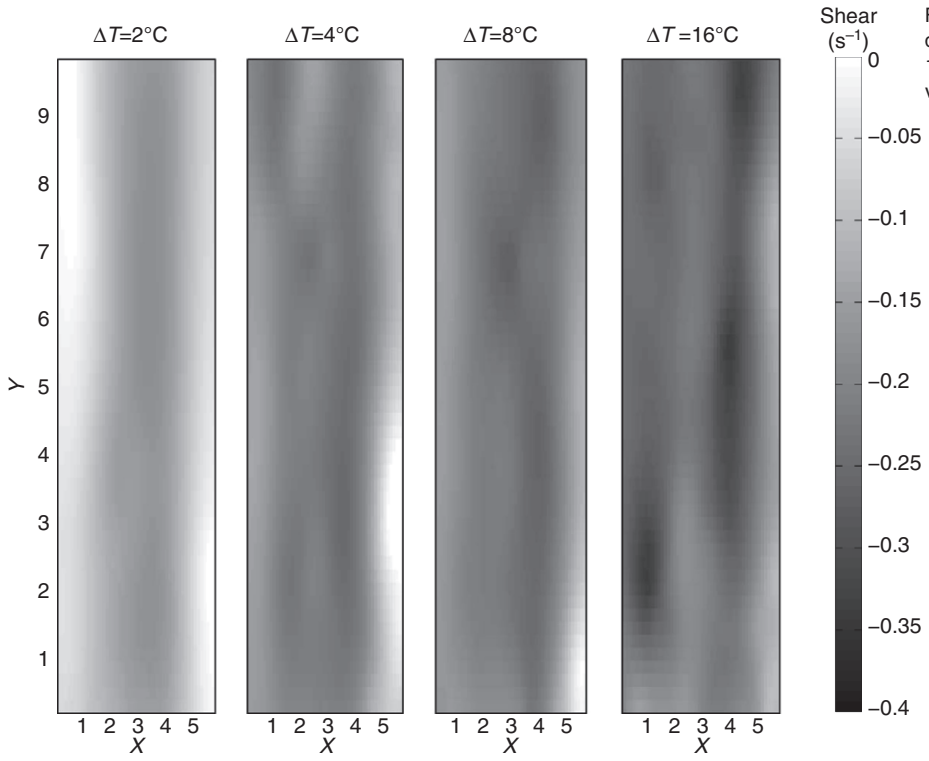

Fig. 5. Shear distribution within the experimental tank driven by temperature differences (Δ*T*) of 2, 4, 8 and 16°C. Shear field was interpolated from binned velocities of tracer particles (see text for details).

respectively; an 8°C difference (7–15°C) resulted in shears of –0.07 to 0.33 s^{-1}; and a 16°C difference (3–19°C) resulted in shears of –0.03 to 0.39 s^{-1} (Fig. 5). The flow in which each larva was instantaneously embedded at each point in its trajectory was determined by interpolation of the PTV-derived velocity field for that shear treatment, using Matlab's thin-plate smoothing spline interpolation function.

This experimental method generated a maximum shear of 0.4 s^{-1}. Therefore, there was overlap between experimental and modeled shears only at the low end of the biologically relevant range.

Larval motion analysis

For each experiment, approximately 50 larvae were added to the experimental tank. Larvae were videotaped for 20 min at each of the three shear regimes (Fig. 4). The width of the imaged field included the center 5.04 mm of the tank. A separate subclip of video was captured and analyzed for each individual larva. Larvae were excluded from the final analysis if they experienced negative shear, if they were imaged within one minute of resuspension, if larval arms were out of focus (indicating the larva was not near the center of the tank) or if the larva was pivoting about one arm or free-falling through the water (indicating non-normal swimming behavior). For larvae that exited and re-entered the field of view or reversed ciliary direction, only the trajectory before the exiting or reversal was included in the analysis.

Data analysis

Because there was overlap between the shears present in the different treatments (Fig. 5), larval tracks were binned into segments of each path falling into three experimental shear ranges: 'low' (0 to 0.2 s^{-1}), 'mid' (0.2 to 0.3 s^{-1}) and 'high' (0.3 to 0.4 s^{-1}). Segments of a single larval track separated into separate shear bins were considered to be separate observations in subsequent analysis. Because our experimental approach did not enable us to identify individual larvae, it is possible that some individual larvae were observed more than once.

For each swimming metric and each larval stage, normality was tested for within each shear bin with the Shapiro–Wilks test, and homogeneity of variances was tested for between shear bins with the Levene test. When these assumptions were met, one-way ANOVAs with Tukey's HSD post-hoc tests were used to test whether each of the swimming metrics differed between shear levels for each larval stage. A harmonic mean was used to account for unequal sample sizes.

Non-parametric statistics were used when analyses included data sets that had non-normal distributions or heterogeneous variances, as transformations did not result in meeting the assumptions of normality or homogeneity of variances. Kruskal–Wallis tests were used to determine whether each of the swimming metrics differed between shear levels for each larval stage. When significant differences were found, Mann–Whitney tests were used to determine whether there were significance differences between each combination of shear levels. A Bonferroni correction was used to reduce the chance of type-one error associated with multiple Mann–Whitney tests on the same data set. Binomial tests were used to examine whether the proportion of larvae moving towards upwelling versus downwelling differed for each shear bin within each stage. All statistical tests were performed with SPSS version 10.0.

RESULTS

Modeling results

All three larval stages in the hydrodynamic model had positive relative vertical velocities at shears below approximately 3 s^{-1} (Fig. 6, Fig. 7A). However, four- and eight-armed larvae were sensitive to moderate or high shear and had negative relative vertical velocities at higher shears. By contrast, six-armed larvae were much more resistant to shear, maintaining an almost constant upward relative vertical velocity up to the highest modeled shear, 10 s^{-1}.

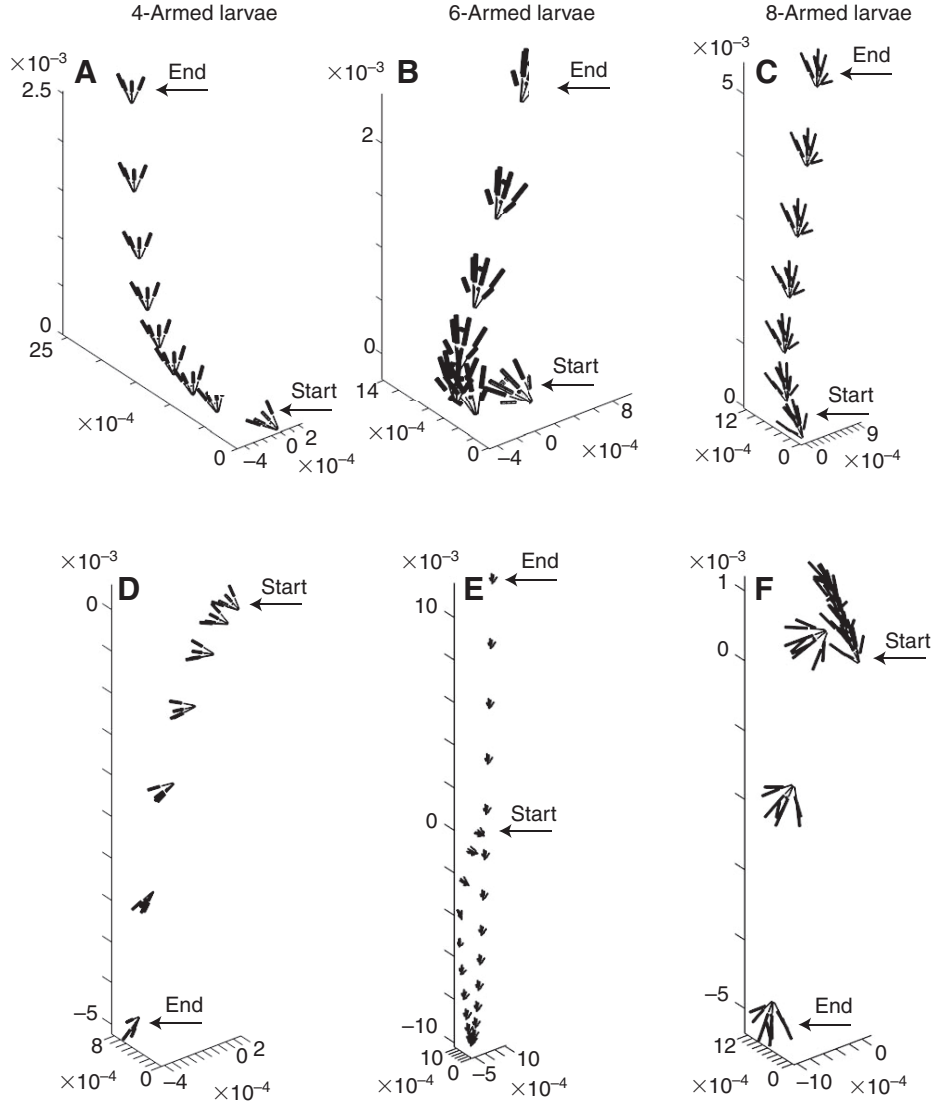

Fig. 6. Examples of modeled larval trajectories in conditions of low vertical shear of 1 s^{-1} (top row) and high vertical shear of 6 s^{-1} (bottom row). All simulations had the same initial orientation and position. The trajectories in this figure vary in duration so as to best illustrate differences in response to flow: (A) 12 s, with snapshots of larval position and orientation taken every 1.5 s, (B and C) 6 s, with snapshots taken every 1 s, (D) 1.5 s, with snapshots taken every 0.25 s, (E) 12 s, with snapshots taken every 0.5 s, and (F) 3 s, with snapshots taken every 0.5 s.

At low shears, all initial orientations of a given stage moved with the same relative vertical velocity, indicating they had adopted a unique stage- and shear-dependent orientation that was independent of their initial orientation. At moderate or high shears, however, all three larval stages showed strong variability in relative vertical velocities, reflected in the broad ranges spanned by the tenth and ninetieth percentiles. This variability indicates that larvae swimming in these stronger shears either had multiple stable orientations, at least some of which rendered the larva unable to support itself in the water column, or suffered an overall loss of stability and persistent tumbling. In both cases, the initial orientation of a modeled larva had significant, long-lasting effects on vertical swimming.

All modeled *Dendraster* larval stages moved into upwelling water in at least some shear flows (Fig. 6, Fig. 8A). This is in contrast to the 'default' horizontal movement by simple shapes such as spheres and ellipsoids, which is always towards downwelling water. In both four- and eight-armed larvae, relative horizontal velocity was directed towards upwelling water at low shears but shifted towards downwelling water at shears of approximately 3 s^{-1} and higher. Six-armed larvae moved faster into upwelling water at low shears than four- and eight-armed larvae. Furthermore, six-armed larvae maintained positive relative horizontal velocities at up to 10 s^{-1}, the highest modeled shear. The magnitude of relative horizontal velocity decreased at the highest shear level for all larval stages, probably reflecting increases in the fraction of time spent tumbling.

At zero shear (no flow), there were no directional hydrodynamic forces that could orient swimming larvae. This was reflected by the spread of horizontal velocities for all three stages at zero shear (Fig. 8A). However, all non-zero modeled levels of shear were sufficient to orient all three larval stages.

For all larval stages, trends in net vertical velocity were qualitatively similar to corresponding trends in relative horizontal and vertical velocities, but quantitatively more exaggerated (Fig. 9A).

Experimental results

The observed larval velocities were highly variable, which might have obscured some underlying trends. In six- and eight-armed larvae, relative vertical velocity differed significantly between shear levels (one-way ANOVA, P=0.043, and Kruskal–Wallis test, P<0.001, respectively; Fig. 7B). In six-armed larvae, relative vertical velocity was greater at high shears than at mid shears (Tukey's HSD post-hoc test, P=0.046; Fig. 7B) but did not vary significantly between low and mid shears or low and high shears (Tukey's HSD post-hoc test, P=0.951 and P=0.103, respectively; Fig. 7B). The relative

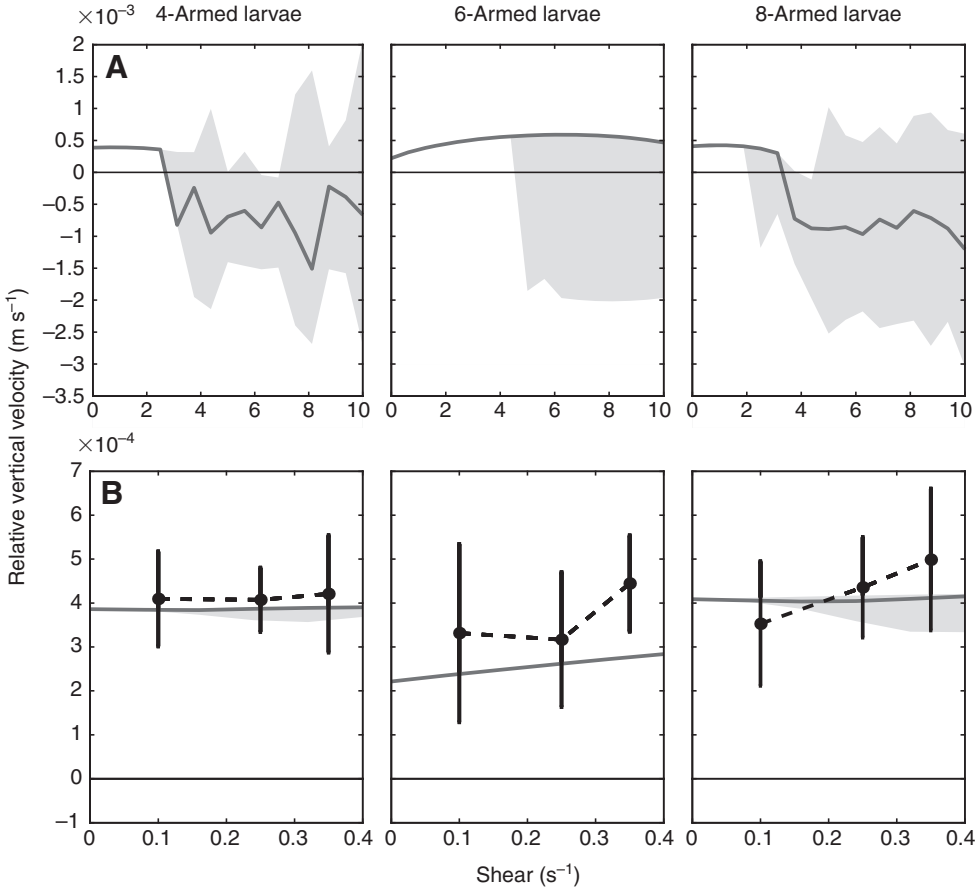

Fig. 7. Relative vertical swimming velocity. (A) Model results for four-, six- and eight-armed larvae are plotted as median relative vertical velocity in vertical shear (dark gray line). The area between the 10th and 90th percentiles is shaded gray; variability in velocity in these regions results from larvae tumbling and/or the existence of multiple stable orientations. (B) A comparison between model and experimental results for four-, six- and eight-armed larvae. Model results for four-, six- and eight-armed larvae are plotted as the median relative vertical velocity in vertical shear (dark gray line) at each of five shear levels ranging from 0 to 0.4 s^{-1}. The 10th and 90th percentiles are plotted as described for row (A). Experimental results are separated by shear bin and plotted as the mean relative vertical velocity (black dashed line), with standard error bars, for four- (N=23 in low shear, 50 in mid shear and 29 in high shear), six- (N=20 in low shear, 24 in mid shear and 16 in high shear) and eight-armed (N=59 in low shear, 72 in mid shear and 32 in high shear) larval stages in vertical shear.

vertical velocities of eight-armed larvae were faster at mid and high shears than at low shears (Mann–Whitney U test, P<0.001 and P<0.001, respectively; Fig. 7B) and were faster at high shears than at mid shears (Mann–Whitney U test, P=0.016; Fig. 7B). In four-armed larvae, relative vertical velocity did not differ significantly between shear levels (Kruskal–Wallis test, P=0.977; Fig. 7B).

In four-armed larvae, the relative horizontal velocity varied significantly with shear, becoming more negative at the highest observed shear level (Kruskal–Wallis test, P=0.001; Fig. 8B). At low shears, four-armed larvae resisted horizontal movement into downwelling water. This contrasted with horizontal velocity at mid and high shears, which was towards downwelling water (Mann–Whitney U test, P=0.002 and P=0.001, respectively; Fig. 8B). The horizontal movement of four-armed larvae did not differ significantly between mid and high shears (Mann–Whitey U test, P=0.149; Fig. 8B). In six- and eight-armed larvae, the relative horizontal velocity was towards downwelling and did not vary significantly between shear levels (one-way ANOVA, P=0.868 and P=0.399, respectively; Fig. 8B).

The proportion of larvae moving towards upwelling versus downwelling water varied with both shear level and larval stage (Fig. 8B). Significantly more four-armed larvae moved towards downwelling than towards upwelling water at mid and high experimental shears (binomial test, P<0.001 and P<0.001, respectively). At low shears, the proportions of four-armed larvae moving into upwelling and downwelling water did not differ (binomial test, P=0.678). By contrast, the proportions of six-armed larvae moving towards upwelling versus downwelling water did not differ at any shear level (binomial test, P=1.000 for low shear, P=0.541 for mid shear, and P=0.454 for high shear). Significantly more eight-armed larvae moved towards downwelling water at all experimental shear levels (binomial test, P<0.001 for low shear, P=0.001 for mid shear, and P=0.020 for high shear).

All stages had upward net vertical velocity at all experimental shears (Fig. 9B). In four-armed larvae, net vertical velocity varied significantly with shear (one-way ANOVA, P=0.001) and was greater at low shear than at mid or high shears (Tukey's HSD post-hoc test, P=0.018 and P<0.001, respectively, when comparing mid and high shears, P=0.180). Net vertical velocities did not differ significantly among shears in six- and eight-armed larvae (Kruskal–Wallis test, P=0.117 and P=0.325, respectively).

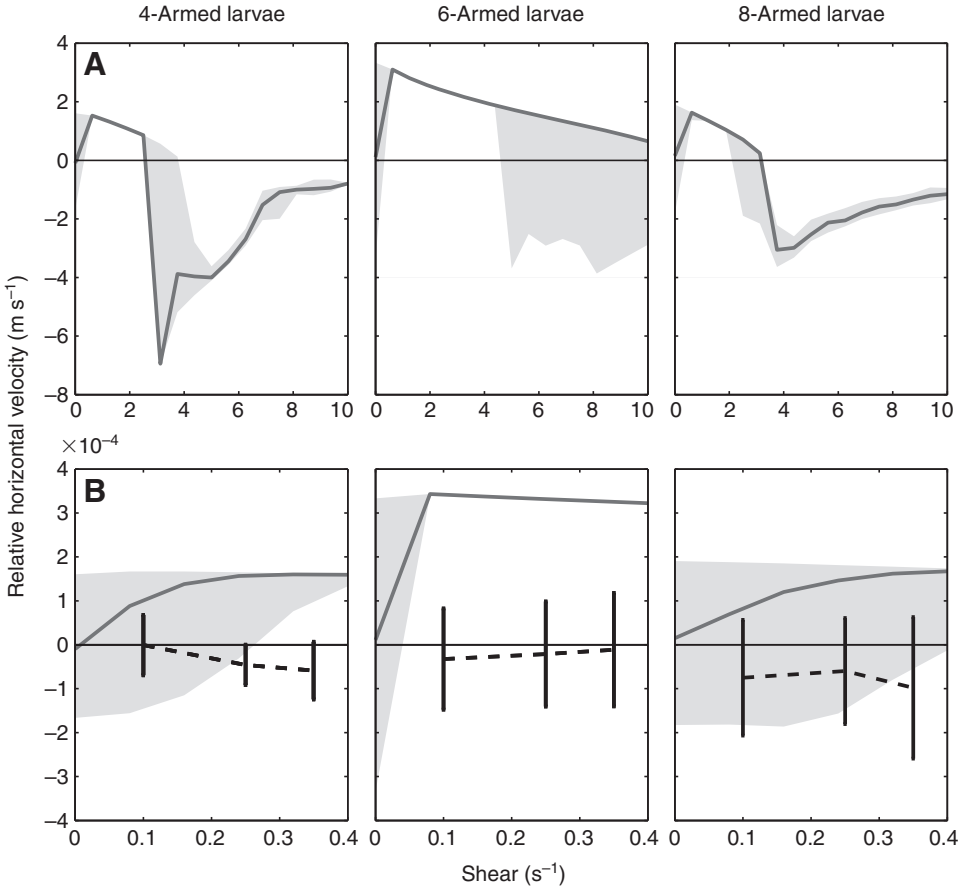

Fig. 8. Relative horizontal swimming velocity. Figure details are as described for Fig. 7.

DISCUSSION

Many larvae and other plankton are conspicuous for their complex and beautiful morphologies. The functional consequences of these morphologies, and their costs and benefits relative to simpler geometries, are in almost all cases poorly understood. We investigated the functional consequences of complex larval morphologies for interactions between planktonic swimming and turbulent water motion. Because larvae are typically smaller than turbulent eddies in estuarine and coastal environments, we approximated turbulent flows as experienced by larvae as a succession of shears that are temporally constant over intervals comparable to Kolmogorov time-scales. We focused on vertical shearing flows (horizontal gradients in vertical velocities) because they are known to exhibit strong hydrodynamic interactions with swimming in planktonic organisms with simpler geometries such as spheres or ellipsoids: vertical shears 'tilt' these organisms, causing them to swim horizontally into downwelling water and compromising their abilities to regulate depth.

We used four-, six- and eight-armed larval stages of the sand dollar *Dendraster excentricus* to ask whether the complex morphologies of these larvae mitigate this deleterious interaction between vertical shears and vertical swimming or even confer an ability to exploit shears to enhance vertical movement. Our key result is both empirical and theoretical evidence suggesting that hydrodynamic interactions between shear and swimming enable *Dendraster* larvae to resist movement into downwelling water and might enable them to move selectively into upwelling water. These results suggest an important element of larval life history in which complex larval morphology has functional significance and potential adaptive advantages over simpler morphologies.

Model results

Model results based closely on observed larval morphologies and low-Reynolds-number theory suggest that *Dendraster* larvae at early (four-armed), middle (six-armed) and late (eight-armed) stages of development all have biased horizontal movement into upwelling water at shear levels typical of calm conditions in estuarine and coastal environments ($\leq$3 s^{-1}). We found qualitative differences between stages in the responses of modeled *Dendraster* larvae to higher environmentally relevant shears up to 10 s^{-1}. Four- and eight-armed model larvae transitioned to downwelling-biased horizontal movements in higher shears, whereas six-armed model larvae maintained an upwelling bias.

We used relative vertical and horizontal velocities – the actual velocities of the larvae minus the velocities of the surrounding water – to quantify larval swimming performance in shear. Like many invertebrate larvae, *Dendraster* larvae swim primarily in a vertical direction in still water. It is not surprising, therefore, that shear-induced relative horizontal velocities in our simulations were substantially smaller than the corresponding relative vertical swimming velocities. Nonetheless, because even small horizontal movements in shear can direct larvae into significant upwelling or downwelling flows, horizontal movements of this magnitude might nonetheless be biologically important.

We devised a performance metric – net vertical velocity – to quantify the combined effects of vertical swimming and horizontal

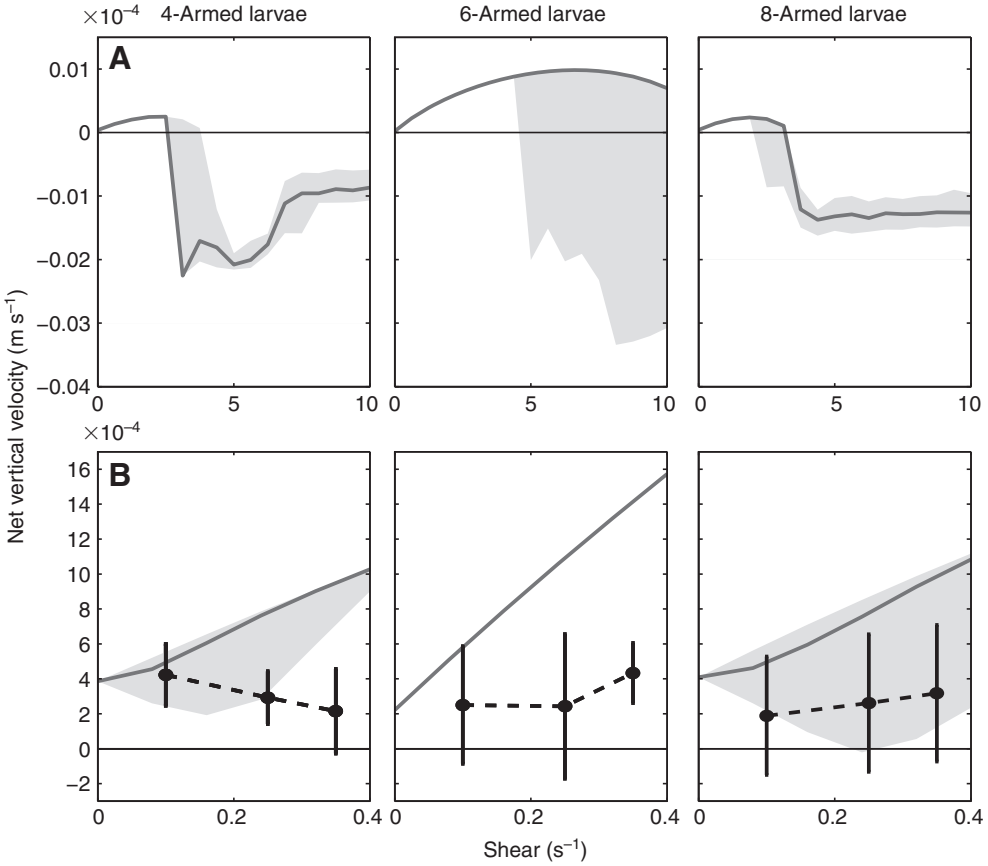

Fig. 9. Net vertical swimming velocity. Figure details are as described for Fig. 7.

movements on larval vertical positions. We calculated this metric for a time interval of 20 s, which falls between the shortest and longest (10^{-1} s and 100 s, respectively) Kolmogorov time-scales for typical oceanic turbulence. In our hydrodynamic simulations, net vertical velocities were substantially larger in magnitude than the corresponding relative vertical velocities. Furthermore, the increase in magnitude occurred at both extremes: up-swimming larvae swam up much faster when horizontal movements were factored in, and downward-moving larvae moved downward much faster. This is theoretical evidence suggesting that horizontal movements, modest though they are, have disproportionate impacts on vertical distributions of *Dendraster* larvae when shear or turbulence is present.

In four- and eight-armed larvae, transitions between maximum positive and negative net velocities occurred over a narrow range of shear levels (*ca*. 2.5–3.5 s^{-1}). Within this range, both the vertical and horizontal velocities of four- and eight-armed larvae changed sign. An interesting outcome of the model was that, beyond this transition, the net vertical velocity in four- and eight-armed larvae remained nearly constant over a threefold increase in shear. Had the horizontal velocities of larvae remained constant over this shear range, downward transport would have also increased three fold over this interval. Instead, the hydrodynamic model suggests that horizontal velocities decrease over this range of shear, almost exactly compensating for the increases in downwards transport. The overall result is to place relatively narrow bounds on the downwards movement of four- and eight-armed larvae in high shear. Thus the model predicts that, through entirely passive means, four- and eight-armed larvae move downwards in above-threshold shear, and do so at a controlled stage-specific rate. If it is assumed that the shear is encountered near the surface, this could be interpreted as an effective built-in mechanism for descending out of energetic surface boundary layers. However, this same mechanism might have the effect of downward transport in bottom boundary layers, where its effects might not be as beneficial to pre-competent larvae.

Comparisons between theory and experiments

Specific comparisons between our observations of *Dendraster* larvae in the thermally driven shear tank and the predictions of the hydrodynamic model were limited by the low maximum shear we could generate in our tank (*ca.* 0.4 s^{-1}). This corresponds to only the lowest fraction of the shear range that we modeled and that larvae are likely to encounter in coastal environments.

Within this narrow range of shears, experimental support for predictions of the model was mixed. We did not observe strong movement into upwelling water. However, we found that four- and eight-armed larvae moved into downwelling water, whereas six-armed larvae did not. Thus, there is both theoretical and empirical support for the finding that the six-armed morphology confers greater resistance to movement towards downwelling water in shear than the four- and eight-armed morphologies.

Several limitations of the model and the experiments might explain the lack of detailed quantitative support of the model results by the experimental results. Simplifications in the model, especially the approximation of arms and other structures as slender cylinders, might have led to imprecise predictions. Our model included only ciliary bands on larval arms, but *Dendraster* and many other armed

larvae also have some ciliation in transverse bands or elsewhere on their bodies. We could not measure some parameters in our model, and so we had to adopt parameters from the literature or adjust them to match the observed swimming characteristics. For example, we assumed that the body volume fraction comprising calcium carbonate was constant across larval stages. If this is incorrect, we likely have inaccuracies in our estimates of gravity and buoyancy forces, and consequently of larval stability. We also lacked direct measurements of the direction of ciliary thrust on larval arms and had to make plausible assumptions. Alternative assumptions might have produced different swimming patterns. In a separate study, we found that *Dendraster* larvae were sensitive to small changes in morphological parameters and that most changes away from observed values were deleterious to larval swimming performance (Clay, 2008) (T.W.C. and D.G., unpublished). We are currently developing a fully three-dimensional model of larval swimming that will circumvent some of these limitations.

In our experiments, larval trajectories exhibited a high degree of variability that might have obscured directional responses in weak shears. Larvae of all stages often swam in spirals in our experiments. We made qualitative observations that larvae continued to swim in spirals even when $MgCl_2$ was used to prevent ciliary reversal, suggesting that spiraling was due, at least in part, to morphology. However, this is in need of quantitative investigation. Bilateral asymmetries between arms within a pair have been observed previously in all stages of larval *Dendraster* (Collin, 1997) (T.W.C. and D.G., unpublished), and these might account for spiral swimming. Rakow and Graham (Rakow and Graham, 2006) found that the scyphomedsa *Aurelia* sp. responded behaviorally to shear by pulsing asymmetrically and that this asymmetry counteracted the rotational effect of shear. It is possible that asymmetry-induced spiral swimming of *Dendraster* plays a functional role in mitigating horizontal biases in shear, but this hypothesis has not yet been investigated. If variability due to small asymmetries was significant at very low shears in our experiments, we predict that experiments at higher shears would be more consistent with our theoretical results. However, we were unable to generate shears that were high enough to test this prediction.

Another possible source of variability in our experiments is larval behavior. Our model assumed that larvae swam as automatons, without active responses to surrounding flows or to their own orientation. Although we excluded distinctly 'non-normal' swimming, such as sinking, reversals and hovering from our analysis, we included less-extreme behavioral variations. In our model, we followed conventional wisdom by assuming that *Dendraster* larvae lack a sensory basis to respond actively to tilting because they have no statoliths or other gravity-sensing organs. However, we hypothesize that these larvae can sense hydrodynamic forces acting on their body and arms and that these forces provide larvae with information on orientation and flow to guide active swimming responses. Six- and eight-armed larvae showed increased swimming speeds in response to increased shear, suggesting a behavioral response to increased shear levels. Similarly, McDonald (McDonald, 2007) found that the swimming speed of *Dendraster* blastulae was greater in higher-shear flows, suggesting that, at this stage, *Dendraster* larvae are also able to sense and respond behaviorally to shear flows.

Despite limitations in both the model and the experiments, both approaches support the overall conclusion that larval movements in vertical shear differ across changes in larval morphology and that some morphologies exist that resist movement into downwelling water. This provides strong evidence that larval morphology–flow interactions are important in terms of larval movement.

Implications for larval development

Six-armed larvae moved into upwelling water consistently across all modeled shear levels. Consequently, upward net vertical velocities were dramatically higher in the modeled six-armed larvae. This is theoretical evidence that modest morphological changes across larval stages have potentially important consequences for swimming performance. An implication is that different stages of *Dendraster* larvae might have different vertical distributions in environments where shear and turbulence are prevalent. Furthermore, it suggests that a larval developmental sequence that consists entirely of upwards-biased or downwards-biased morphologies might hypothetically be possible.

What is the selective value of upwards versus downwards movement changes between stages? A possibility is that different depths might confer different advantages and disadvantages upon different larval stages. Another hypothesis is that the presence of larval stages that move downward in shear might result from larvae adopting unfavorable morphologies at some stages because they are necessary intermediates between earlier and later stages. Alternatively, swimming performance might be compromised at some or all of these stages by other, more dominant, selective factors, such as feeding or predator avoidance.

Although these hypotheses have not yet been addressed directly, some insights are offered by changes in the symmetry of larvae as they progress from four- to six- to eight-armed stages. All *Dendraster* stages are approximately bilaterally symmetrical, albeit with small asymmetries, until development of the juvenile rudiment (Collin, 1997). Both four- and eight-armed larvae are additionally close to dorso-ventrally symmetric (and thus nearly four-fold symmetrical). In still water, four-fold-symmetrical larvae have no horizontal velocity. By contrast, six-armed larvae have bilateral symmetry but strong dorso-ventral asymmetries that confer a horizontal component even in still water. In the hydrodynamic model, the six-armed morphology interacted with shear flows to orient larvae such that this horizontal component was predominately in the upwelling direction. Because the model included no active responses to position or surrounding flow, this can only be due to the morphological characteristics of this larval stage.

The transition from four-fold to bilateral and then back to four-fold symmetries results from the timing of growth in specific pairs of arms during larval development. Larvae progress from the four-armed to the six-armed stage with the appearance of the third pair of arms, the posterodorsal arms. These arms grow in approximately the same plane as the anterolateral arms. The fourth pair of arms, the preoral arms, also appears at this stage. However, they remain as small, undeveloped stubs through the six-armed stage. Growth of this fourth arm pair marks the transition from the six- to the eight-armed stage, and the beginning of a transition back towards four-fold symmetry. The morphology of the eight-armed larva modeled as part of this study represents a dramatic reduction in dorso-ventral asymmetry when compared with the six-armed larva. This reduction in dorso-ventral asymmetry continues as the larva progresses through the eight-armed stage, and larvae in more advanced eight-armed stages more nearly approach four-fold symmetry [e.g. figure 1 in Grünbaum and Strathmann (Grünbaum and Strathmann, 2003)]. Thus, while it is not possible to identify the costs and benefits of movement into upwelling or downwelling water, the model suggests that differences in horizontal movement among four-, six- and eight-armed stages are primarily due to sequential, rather than simultaneous, development of the third and fourth pairs of arms. As there is no obvious developmental constraint that would prevent simultaneous growth, the leading explanation appears to be that

sequential development is selectively advantageous, either for locomotion or for some other function.

Evolution of larval morphology is shaped by many factors, some of which reflect immediate costs and benefits and others that potentially reflect longer-term phylogenetic or developmental constraints or limits. 'Armed' larvae, which possess long thin ciliated protrusions for propulsion and feeding, define a morphological theme that arises frequently across diverse marine invertebrate taxa. Armed larvae share essential elements of body plan and locomotory mechanism, but they are also highly variable across and within species in terms of number, position, geometry and stiffness of arms. Presently, little is known about the functional advantages or disadvantages of armed larval morphologies relative to other larval designs, the costs and benefits of geometric variations among the armed larvae or the constraints on performance imposed on some larval stages by the need for developmental continuity with earlier and later stages.

The high degree of morphological variability within the 'armed' larvae suggests multiple hypotheses regarding the effect of morphology on larval swimming. Larval morphology might vary because swimming performance is so insensitive to moderate changes in morphology that other selective forces, such as feeding, are the primary influences on larval morphology. In our models and experiments, relatively small changes in size and orientation of arms in transition from six- to eight-armed larval stages resulted in qualitatively and quantitatively different swimming performance. These results appear inconsistent with insensitivity to morphology but consistent with a second hypothesis: swimming performance might be strongly sensitive to larval morphology, to the point where diverse morphological characters must be 'tuned' simultaneously to produce viable morphologies. If so, changes in one geometric parameter would require commensurate changes in many others in a manner that might strongly constrain developmental mechanisms. The differences we observed in swimming performance between four-, six- and eight-armed *Dendraster* larvae support the second, higher-sensitivity, interpretation.

Future marine environments are likely to be impacted by anthropogenic changes. If, owing to anthropogenic influences, environments differ from those in which larvae such as *Dendraster* evolved, there is little reason to be confident that larvae will maintain the tight geometrical coupling needed to maintain swimming performance. For example, acidification at levels predicted by the Intergovernmental Panel on Climate Change (IPCC) has been found to alter the morphologies of larval echinoderms (Kurihara, 2008). If, as suggested by this study, small changes in larval morphology have large consequences for swimming, then environmental changes that impact larval morphology might have subtle, but significant, indirect effects that disrupt large-scale patterns of connectivity in many adult marine invertebrate populations.

ACKNOWLEDGEMENTS

We thank Richard Strathmann for insight and advice throughout this work. We also thank Terrie Klinger, Bruce Frost, Parker MacCready and Kathryn McDonald for advice and Dianna Padilla for comments that greatly improved this manuscript. Much of this work was completed at the University of Washington's Friday Harbor Laboratories. We gratefully acknowledge support by the Stephen and Ruth Wainwright Endowed Fellowship awarded to T.W.C. and by the National Science Foundation, Grant OCE-0220284, to D.G.

REFERENCES

Bearon, R. N. and Grünbaum, D. (2006). Bioconvection in a stratified environment: experiments and theory. *Phys. Fluids* **18**, 127102

Boidron-Metairon, I. F. (1988). Morphological plasticity in laboratory-reared echinoplutei of *Dendraster excentricus* (Eschscholtz) and *Lytechinus variegatus* (Lamarck) in response to food conditions. *J. Exp. Mar. Biol. Ecol.* **119**, 31-41.

Burns, N. M. and Rosa, F. (1980). In situ measurement of the settling velocity of organic carbon particles and 10 species of phytoplankton. *Limnol. Oceanogr.* **25**, 855-864.

Chia, F. S., Bucklandnicks, J. and Young, C. M. (1984). Locomotion of marine invertebrate larvae: a review. *Can. J. Zool.* **62**, 1205-1222.

Clay, T. W. (2008). Effects of morphology and flow on the swimming performance and dispersal of pelagic larvae of the sand dollar *Dendraster excentricus*. Ph.D. dissertation, University of Washington.

Collin, R. (1997). Ontogeny of subtle skeletal asymmetries in individual larvae of the sand dollar *Dendraster excentricus*. *Evolution* **51**, 999-1005.

Cowen, R. K. and Sponaugle, S. (2009). Larval dispersal and marine population connectivity. *Ann. Rev. Mar. Sci.* **1**, 443-466.

Durham, W. M., Kessler, J. O. and Stocker, R. (2009). Disruption of vertical motility by shear triggers formation of thin phytoplankton layers. *Science* **323**, 1067-1070.

Emlet, R. B. (1990). Flow-fields around ciliated larvae: effects of natural and artificial tethers. *Mar. Ecol. Prog. Ser.* **63**, 211-225.

Emlet, R. B. (1991). Functional constraints on the evolution of larval forms of marine invertebrates: experimental and comparative evidence. *Am. Zool.* **31**, 707-725.

Emlet, R. B. (1994). Body form and patterns of ciliation in nonfeeding larvae of echinoderms: functional solutions to swimming in the plankton? *Am. Zool.* **34**, 570-585.

Fuchs, H. L., Mullineaux, L. S. and Solow, A. R. (2004). Sinking behavior of gastropod larvae (*Ilyanassa obsoleta*) in turbulence. *Limnol. Oceanogr.* **49**, 1937-1948.

Grünbaum, D. and Strathmann, R. R. (2003). Form, performance and trade-offs in swimming and stability of armed larvae. *J. Mar. Res.* **61**, 659-691.

Hadfield, M. G. and Koehl, M. A. R. (2004). Rapid behavioral responses of an invertebrate larva to dissolved settlement cue. *Biol. Bull.* **207**, 28-43.

Hart, M. W. and Strathmann, R. R. (1994). Functional consequences of phenotypic plasticity in echinoid larvae. *Biol. Bull.* **186**, 291-299.

Higgins, J. E., Ford, M. D. and Costello, J. H. (2008). Transitions in morphology, nematocyst distribution, fluid motions, and prey capture during development of the scyphomedusa *Cyanea capillata*. *Biol. Bull.* **214**, 29-41.

Hunt, A. (1993). Effects of contrasting patterns of larval dispersal on the genetic connectedness of local populations of two intertidal starfish, Patiriella calcar and P. exigua. *Mar. Ecol. Prog. Ser.* **92**, 179-186.

Kessler, J. O. (1985). Hydrodynamic focusing of motile algal cells. *Nature* **313**, 218-220.

Kiøerboe, T. and Saiz, E. (1995). Planktivorous feeding in calm and turbulent environments, with emphasis on copepods. *Mar. Ecol. Prog. Ser.* **122**, 135-145.

Koehl, M. A. R. and Reidenbach, M. A. (2007). Swimming by microscopic organisms in ambient water flow. *Exp. Fluids* **43**, 755-768.

Kundu, P. K. and Cohen, I. M. (2002). *Fluid Mechanics*. San Diego, CA: Academic Press.

Kurihara. H. (2008). Effects of CO_2-driven ocean acidification on the early developmental stages of invertebrates. *Mar. Ecol. Prog. Ser.* **373**, 275–284.

McDonald, K. A. (2007). Early embryonic motility in broadcast-spawning marine invertebrates: ciliary swimming, risk, and migration in the plankton Ph.D. dissertation, University of Washington.

McEdward, L. R. (1984). Morphometric and metabolic analysis of the growth and form of an echinopluteus. *J. Exp. Mar. Biol. Ecol.* **82**, 259-287.

McEdward, L. R. and Herrera, J. C. (1999). Body form and skeletal morphometrics during larval development of the sea urchin *Lytechinus variegatus* (Lamarck). *J. Exp. Mar. Biol. Ecol.* **232**, 151-176.

McHenry, M. J. (2005). The morphology, behavior, and biomechanics of swimming in ascidian larvae. *Can. J. Zool.* **83**, 62-74.

Pawlik, J. R. and Butman, A. C. (1993). Settlement of a marine tube worm as a function of current velocity: interacting effects of hydrodynamics and behavior. *Limnol. Oceanogr.* **38**, 1730-1740.

Pedley, T. J. and Kessler, J. O. (1992a). Bioconvection. *Sci. Prog.* **76**, 105-123.

Pedley, T. J. and Kessler, J. O. (1992b). Hydrodynamic phenomena in suspensions of swimming microorganisms. *Annu. Rev. Fluid Mech.* **24**, 313-358.

Pennington, J. T. and Emlet, R. B. (1986). Ontogenetic and diel vertical migration of a planktonic echinoid larva, *Dendraster excentricus* (Eschscholtz): occurrence, causes, and probable consequences. *J. Exp. Mar. Biol. Ecol.* **104**, 69-95.

Pennington, J. T. and Strathmann, R. R. (1990). Consequences of the calcite skeletons of planktonic echinoderm larvae for orientation, swimming, and shape. *Biol. Bull.* **179**, 121-133.

Rakow, K. C. and Graham, W. M. (2006). Orientation and swimming mechanics by the scyphomedusa Aurelia sp. in shear flow. *Limnol. Oceanogr.* **51**, 1097-1106.

Scheltema, R. S. (1986). Long-distance dispersal by planktonic larvae of shoal-water benthic invertebrates among central Pacific islands. *Bull. Mar. Sci.* **39**, 241-256.

Shanks, A. L., Grantham, B. A. and Carr, M. H. (2003). Propagule dispersal distance and the size and spacing of marine reserves. *Ecol. Appl.* **13**, S159-S169.

Sheng, J., Malkiel, E., Katz, J., Adolf, J., Belas, R. and Place, A. R. (2007). Digital holographic microscopy reveals prey-induced changes in swimming behavior of predatory dinoflagellates. *Proc. Natl. Acad. Sci. USA* **104**, 17512-17517.

Strathmann, M. F. (1987). *Reproduction and Development of Marine Invertebrates of the Northern Pacific Coast*. Seattle, WA: University of Washington Press.

Strathmann, R. R. and Grünbaum, D. (2006). Good eaters, poor swimmers: compromises in larval form. *Integr. Comp. Biol.* **46**, 312-322.

Tennekes, H. and Lumley, J. L. (1972). *A First Course in Turbulence*. Cambridge, MA: The MIT Press.

Yamazaki, H., Mackas, D. L. and Denman, K. L. (2002). Coupling small-scale physical processes with biology. In *The Sea*, vol. 12 (ed. A. R. Robinson J. J. McCarthy and B. J. Rothschild), pp. 51-112. New York: John Wiley & Sons, Inc.

Young, C. M., Sewell, M. A., Rice, M. E. (2002). *Atlas of Marine Invertebrate Larvae*. New York, NY: Academic Press.